

Discovery of a Potent and Selective TRPC5 Inhibitor, Efficacious in a Focal Segmental Glomerulosclerosis Model

Maolin Yu, Mark W. Ledeboer, Matthew Daniels, Goran Malojcic, Thomas
T Tibbitts, Marie Coeffet-Le Gal, Xin-Ru Pan-Zhou, Amy Westerling-Bui,
Maria Beconi, John F Reilly, Peter Mundel, and Jean-Christophe Harmange

ACS Med. Chem. Lett., **Just Accepted Manuscript** • DOI: 10.1021/acsmchemlett.9b00430 • Publication Date (Web): 22 Oct 2019

Downloaded from pubs.acs.org on October 26, 2019

Just Accepted

“Just Accepted” manuscripts have been peer-reviewed and accepted for publication. They are posted online prior to technical editing, formatting for publication and author proofing. The American Chemical Society provides “Just Accepted” as a service to the research community to expedite the dissemination of scientific material as soon as possible after acceptance. “Just Accepted” manuscripts appear in full in PDF format accompanied by an HTML abstract. “Just Accepted” manuscripts have been fully peer reviewed, but should not be considered the official version of record. They are citable by the Digital Object Identifier (DOI®). “Just Accepted” is an optional service offered to authors. Therefore, the “Just Accepted” Web site may not include all articles that will be published in the journal. After a manuscript is technically edited and formatted, it will be removed from the “Just Accepted” Web site and published as an ASAP article. Note that technical editing may introduce minor changes to the manuscript text and/or graphics which could affect content, and all legal disclaimers and ethical guidelines that apply to the journal pertain. ACS cannot be held responsible for errors or consequences arising from the use of information contained in these “Just Accepted” manuscripts.

Discovery of a Potent and Selective TRPC5 Inhibitor, Efficacious in a Focal Segmental Glomerulosclerosis Model

Maolin Yu,^{*,†} Mark W. Ledebner,^{*,†} Matthew Daniels,[†] Goran Malojcic,[†] Thomas T. Tibbitts,[†] Marie Coeffet-Le Gal,[#] Xin-Ru Pan-Zhou,[#] Amy Westerling-Bui,[#] Maria Beconi,^{#,v} John F. Reilly,[#] Peter Mundel,[#] and Jean-Christophe Harmange[†]

[†]Drug Discovery, [#]Biology, Goldfinch Bio Inc., Cambridge, Massachusetts 02142, United States

KEYWORDS: TRPC5, focal segmental glomerulosclerosis, DOCA, podocyte, proteinuria, kidney disease

ABSTRACT: The non-selective Ca²⁺-permeable Transient Receptor Potential (TRP) channels play important roles in diverse cellular processes, including actin remodeling and cell migration. TRP channel subfamily C, member 5 (TRPC5) helps regulate a tight balance of cytoskeletal dynamics in podocytes and is suggested to be involved in the pathogenesis of proteinuric kidney diseases, such as focal segmental glomerulosclerosis (FSGS). As such, protection of podocytes by inhibition of TRPC5 mediated Ca²⁺ signaling may provide a novel therapeutic approach for the treatment of proteinuric kidney diseases. Herein, we describe the identification of a novel TRPC5 inhibitor, **GFB-8438**, by systematic optimization of a high-throughput screening hit, pyridazinone **1**. **GFB-8438** protects mouse podocytes from injury induced by protamine sulfate (PS) *in vitro*. It is also efficacious in a hypertensive deoxycorticosterone acetate (DOCA)-salt rat model of FSGS, significantly reducing both total protein and albumin concentrations in urine.

Progressive chronic kidney disease (CKD) is a global health concern, affecting over 500 million people worldwide and about 26 million in US alone.^{1,2} CKD is regarded as an accelerator of cardiovascular disease (CVD), which, along with renal failure are the primary cause of morbidity and mortality in this underserved population.³ As one of the leading causes of glomerular disease, focal segmental glomerulosclerosis (FSGS) in its most severe form is associated with the nephrotic syndrome characterized by symptomatic proteinuria (> 3.5 g protein per day) in adults, scarring of the glomerulus, and loss of terminally differentiated podocytes.^{4,5} Currently there are few effective treatments for FSGS and many patients are treated chronically with steroids, which have undesirable side effects. Therefore, there is a significant unmet need for novel therapeutic approaches that can prevent or slow disease progression.

A hallmark of the pathogenesis of FSGS is podocyte injury and loss. Podocyte foot process effacement, one of the first morphologic alterations of the glomerular filtration barrier, is caused by the disruption of the podocyte actin cytoskeleton via activation of Rac1.⁶ TRPC5 has been identified as a key mediator of Rac1 activation in podocytes.^{7,8} TRPC5 belongs to the mammalian superfamily of transient receptor potential (TRP) Ca²⁺-permeable non-selective cationic channels.⁹ Damage to podocytes activates Rac1, leading to translocation of TRPC5 to the cell membrane. Activation of the membrane-located

TRPC5 channel leads to further Rac1 activation in a feed-forward loop, thereby driving cytoskeletal remodeling. The ensuing cytoskeletal changes lead to effacement of podocyte foot processes, podocyte loss and proteinuria. Inhibition of TRPC5 by small molecules has been shown to protect podocytes *in vitro* and suppresses proteinuria and podocyte loss *in vivo*, in a transgenic rat model of FSGS.^{10,11} TRPC5-knockout (KO) mice were also protected from lipopolysaccharide (LPS)-induced albuminuria.¹⁰ Collectively, these results suggest that inhibition of TRPC5 may provide a novel, effective and safe approach for the treatment of FSGS and related proteinuric kidney diseases.

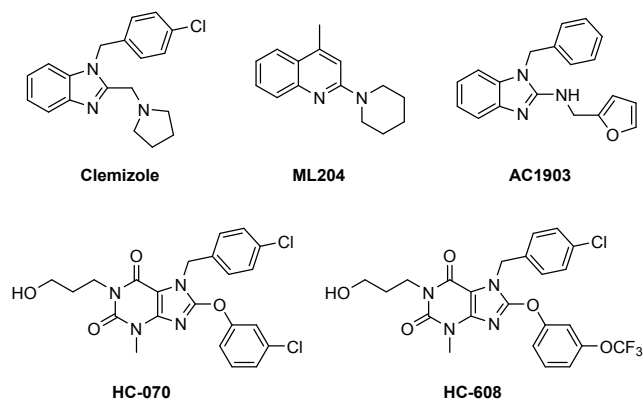
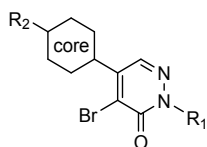
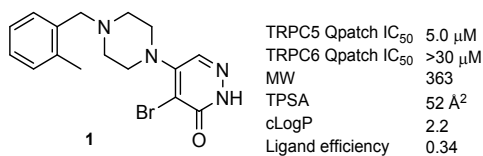


Figure 1. Representative TRPC5 inhibitors from the literature.

Table 1. Summary of early dynamic SAR and core modification

Cmpd	R ₂	Cores	R ₁	TRPC5 Qpatch IC ₅₀ (μM) ^a	Cmpd	R ₂	Cores	R ₁	TRPC5 Qpatch IC ₅₀ (μM) ^a
1			H	5.0	9			H	1.9
2			H	18	10			H	>30
3			H	8.0	11			H	>30
4			H	8.8	12			H	0.50
5			H	1.8	13			H	>30
6-1 ^c			H	16	14			H	27
6-2			H	>30	15			H	>30
7			Me	27	16			H	>30
8				>30	17			H	2.8

^a Qpatch assay measuring the outward current at +80 mV in HEK 293 cells overexpressing human TRPC5 activated by 30 μM Rosiglitazone. Results are mean of at least two experiments. Experimental errors within 30% of value. ^bThis denotes the end connecting to pyridazinone. ^cChloro analogue.

**Figure 2. HTS hit, 1**

Several subtype-selective small molecule TRPC5 inhibitors have recently emerged in the literature.^{12,13,14} The structures of representative compounds are summarized in Figure 1. Chemical probes such as ML204,¹⁵ Clemizole,¹⁶ and AC1903¹⁷ have been instrumental in understanding the biological roles of TRPC5. In addition, this pioneering work helped to underscore the therapeutic potential associated with its inhibition. Although effective as molecular probes, these molecules generally suffer from low potency, off-target activities or unknown selectivity and unfavorable pharmacokinetic properties. However, xanthine analogues such as HC-608 and HC-070,

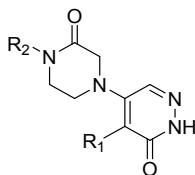
identified by Hydra/Boehringer-Ingelheim, are highly potent.¹⁸ While these compounds have further helped advance TRPC4 and TRPC5 biology, especially in the CNS, this series of inhibitors suffers from poor physicochemical properties such as low solubility (kinetic solubility of HC-608 is 0.03 μM at pH 7.4 in phosphate buffer) and very high protein binding (>99.5% bound). In our search for novel TRPC5 inhibitors with an improved overall profile, we screened a structurally diverse library of ~400,000 compounds against TRPC5, using a FLIPR assay, which resulted in the identification of several low micromolar hits. From the hit set, pyridazinone **1** (Figure 2) was selected as an attractive starting point for further exploration based on the encouraging potency, selectivity over TRPC6, good ligand efficiency, low cLogP as well as the potential for rapid SAR exploration. Another important consideration was the ability of **1** to block the TRPC5 channel with similar potency, independent of the activators used (Rosiglitazone A: IC₅₀ 5.0 μM, Riluzole: IC₅₀

7.8 μM , (-)-Englerin A: IC_{50} 4.0 μM , and Lanthanum: IC_{50} 4.4 μM).

Our initial chemistry efforts focused on the improvement of the potency in blocking TRPC5 channel Ca^{2+} current. A survey of benzylic groups indicated dynamic SAR and suggested the possibility of improving potency. As exemplified by compounds **1**, **2** and **3** (Table 1),

aromatic and aliphatic R_2 groups were tolerated. However, incorporation of heteroaromatic groups tended to lead to erosion of potency as represented by **6-1,6-2**, **34** and **36**. As shown by **5**, addition of a *p*-fluoro group boosted potency 2.5x relative to compound **1**, while removal of the *o*-Me group led to a 3x loss in potency. Racemic methyl substitution on benzylic methylene was tolerated (**4**). Turning our

Table 2. Summary of SAR in Br and benzyl region



Compd	R ₁	R ₂	TRPC5 Qpatch IC_{50} (μM)	Compd	R ₁	R ₂	TRPC5 Qpatch IC_{50} (μM) ^a
12	-Br		0.5	28	-Cl		14.5
18	-Me		28.0	29	-Cl		0.38
19	-Et		11.0	30	-Cl		0.49
20	-iPr		2.4	31	-Cl		0.65
21	*		1.5	GFB-8438	-Cl		0.18
22	*		>30	32	-Cl		0.53
23	-Cl		0.66	33	-Cl		>30
24	-CF ₃		9.6	34	-Cl		11.2
25	-CN		1.9	35	-Cl		0.65
26	-OMe		>30	36	-Cl		8.2
27	*		>30	37	-Cl		0.53
				38	-Cl		>30

^aResults are mean of at least two experiments. Experimental errors within 30% of value. Activated (by 30 μM Rosiglitazone) TRPC5 overexpressed HEK 293 cells used for outward current measurement at +80 mV in Qpatch assay.

attention to the pyridazinone ring, methylation and alkylation of the NH as in **7** and **8** respectively greatly diminished the TRPC5 potency, suggesting that the NH may be involved in a productive H-bond. Investigation of modifications to the piperazine core proved informative. Introduction of a chiral Me group provided enantiomers with divergent activities as in **9** vs **10**. However, methylation adjacent to the basic piperazine N, as in **11**, led to ablation of all potency. As demonstrated with **13**, replacing the basic N with carbon resulted in complete loss

		8438	32	35
HT-solubility (pH = 7.4) (μ M)		316	114	12
rLM/hepatocyte	CL _{int}	24 / 94	55 / 147	18 / 26
hLM/hepatocyte	CL	7.8 / 5.5	0.14 / 4.1	4.3 / 5.3
Pharmacokinetics		rat	rat	rat
CL (mL/min/kg)		31	56	27
T _{1/2} (h)		0.50	0.45	1.05
V _{ss} (L/Kg)		1.17	1.27	1.81
F (PO/SC) (%)		17 / 33	19 / -	22 / -

of potency. Homopiperazine (**14**) exhibited diminished activity as well. Attempts to introduce bridged and spiro features to the piperazine ring turned out to be unproductive (**15**, **16**), except analogue **17**, which has comparable activity to **1**, but with much less favored physicochemical properties. Interestingly, introduction of the lactam carbonyl saw a 10x fold boost in potency (**12**). Contrasting to the basic nature of the piperazine core, the lactam displays very distinct electrostatic properties. The switch from sp³ to sp² also results in conformational and trajectory change for piperazine and the adjacent benzyl group (See Figure S1 for modelling study). These highly specific SAR suggests that piperazine might sit in a well-defined binding pocket and the potency gain observed with the lactam is indicative of productive interactions with the protein.

Owing to the potential instability we turned our attention to the bromide functionality in this series. We speculated that it may play multiple roles: a) halogen bonding with protein residue; b) fine tuning of the pKa of the acidic proton in the warhead; c) steric and conformational constraint of piperazinone scaffold. As such, we replaced the Br with groups of varying size and polarity. Replacing Br with a methyl (**18**) afforded measurable potency. Increasing the alkyl size (**18** to **21**) led to the increase in inhibitory activity with cyclopropyl as the most optimal. However, larger groups such as THP were not tolerated (**22**). Unsurprisingly, Cl analogue (**23**) yielded similar potency to **12**. Small electron-withdrawing substituents were also tolerated albeit with 4- to 20-fold reduction in potency (**24**, **25**). Electron-donating substitution (**26**, **27**) proved to be ineffective, hinting at the need to maintain pKa of the acidic NH proton. Through this effort, we identified Cl as a suitable replacement for Br, which is a common element in many approved medicines.¹⁹

Having addressed several shortcomings related to the original hit, the potency for blocking the Ca⁺² current still had room for further improvement (Table 2). Walking methyl around the phenyl ring established that the ortho mono-methyl substitution is most effective (**23**, **28**, **29**, **30**). Based on this result, we screened a range of ortho-substituted analogues in order to identify a group to further improve the potency and balance physicochemical properties and microsomal stability. SAR suggested lipophilic groups in this position were well tolerated with CH₃, Cl or CF₃ (**23**, **31**, **32**, **GFB-8438**). While incorporating nitrogen next to CF₃ (**34**) improved the properties, it led to dramatic loss in activity. Substitution in the para-position with F to block the potential metabolic soft spot caused slight erosion in potency (**35**). Polar motifs (**33**, **36**, **38**) showed potency loss trend as well, suggesting this part of the compound might bind in a lipophilic pocket. Indeed 4-Me-cyclohexyl (**37**) was equally potent as **23**, but unfortunately with very unfavorable physicochemical properties.

Table 3. DMPK Profiling of GFB-8438, 32 and 35^a

^aSee Supporting Information for experimental details.

Several analogues identified in Table 2 have reasonable potencies and potential to serve as tool compounds for *in vivo* study. As such we determined the PK parameters for **GFB-8438**, **32**, and **35** (Table 3). All three compounds demonstrated good metabolic stability when incubated with both human liver microsomes and hepatocytes, but with less stability in rat. The observed intrinsic microsomal clearance correlated well with *in vivo* rat clearance, and oral bioavailability in rats was modest and similar for each of the three compounds. When dosed subcutaneously, **GFB-8438** exhibited significantly higher plasma exposure. With the subcutaneous route overcoming the limited oral bioavailability, **GFB-8438** was deemed suitable for dosing in our efficacy model.

Table 4. *in vitro* profile of GFB-8438^a

hTRPC5 Qpatch IC ₅₀ (μ M)	0.18
hTRPC5 manual patch clamp IC ₅₀ (μ M)	0.28
rTRPC5 Qpatch IC ₅₀ (μ M)	0.18
hTRPC4 Qpatch IC ₅₀ (μ M)	0.29
hTRPC6 Qpatch IC ₅₀ (μ M)	>30
Nav1.5 manual patch clamp IC ₅₀ (μ M)	>30
hERG manual patch IC ₅₀ (μ M)	8.7
Eurofins kinase panel (%Ctrl @10 μ M)	>50 (LOK 33%)
Eurofins receptor panel (%inh @10 μ M)	All < 50%
Equilibrium Solubility (pH=7.4) (μ M)	48
Human plasma protein binding (%)	69
MDCK-MDR1 P _{A-B} /ER (10 ⁻⁶ cm/s)	20 / 1.6

^aSee Supporting Information for experimental details.

Having achieved a desired pharmacokinetic profile in rat, we embarked on further characterizing **GFB-8438**. We first confirmed the inhibition of human TRPC5 by manual patch clamp. **GFB-8438** inhibited the whole cell current with an IC₅₀ of 0.28 μM comparable to the IC₅₀ in Qpatch assay (0.18 μM) (Table 4). We then determined the potency of **GFB-8438** against the TRPC5 rat ortholog and found it is equally potent in rodent TRPC5 Qpatch assay. Screening for activity against a panel of TRP channels, we also found that **GFB-8438** was equipotent against TRPC4 and TRPC5, and showed excellent selectivity against TRPC6, other TRP family members (such as TRPC3/7, TRPA1, TRPV1/2/3/4/5 and TRPM2/3/4/8, data not shown), NaV 1.5, as well as limited activity against the hERG channel. In addition, **GFB-8438** did not display significant off-target activity

when screened against the safety panels of kinases (59 kinases) and receptors (87 targets).

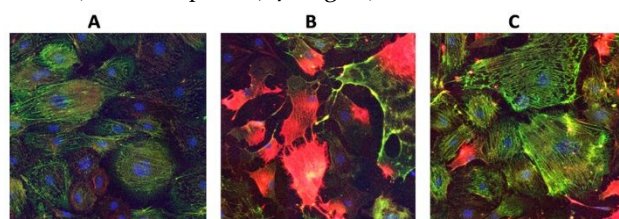


Figure 3. *in vitro* efficacy study for **GFB-8438** in PS-induced mouse podocytes injury assay. (A) Control mouse podocytes without PS and **GFB-8438**; (B) Mouse podocytes after treatment with PS (300 μM for 15 min); (C) Mouse podocytes pretreated with **GFB-8438** (1 μM for 30 min), then insulted with PS. The tiled images were acquired using a Zeiss LSM880 Airyscan super resolution confocal microscope. Green color: Synaptopodin; Red color: Phalloidin; Blue color: Dapi.

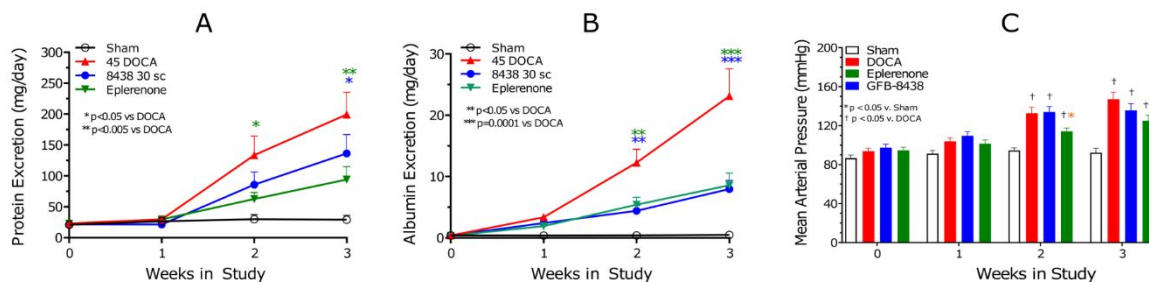


Figure 4. *in vivo* efficacy study for **GFB-8438** in DOCA rat model (n = 8 in sham group, n = 15 in all other groups). Sprague Dawley rats were unilaterally nephrectomized; after one-week recovery, rats were implanted with a DOCA pellet (45 mg) and provided with high salts-containing tap water for 3 weeks of treatment. DOCA-salt rats received once daily subcutaneous of **GFB-8438** at 30 mg/kg or twice daily oral dosing of eplerenone at 50 mg/kg for 3 weeks. Hemodynamic parameters and urinary albumin and protein were measured weekly. (A) total urinary protein excretion at week 0, 1, 2 and 3; (B) total urinary albumin excretion at week 0, 1, 2 and 3; (C) Mean arterial blood pressure measured at week 0, 1, 2 and 3. No difference in creatinine clearance cross all groups. Data are presented as mean ± SEM.

Based on the observed potency, selectivity, the overall favorable physicochemical properties, and PK profile, **GFB-8438** was selected as an attractive tool compound for further testing in *in vitro* and *in vivo* efficacy studies.

Thus, we sought to assess the ability of **GFB-8438** to elicit protective effect on podocytes following injury induced by protamine sulfate (PS).^{10,20,21} Conditionally immortalized mouse podocytes were incubated with PS, an indirect activator of TRPC5. Extensive actin disruption and loss of stress fibers was observed as demonstrated by the loss of synaptopodin and a reorganization of the phalloidin stained actin cytoskeleton (Figure 3, B). In contrast, pretreatment of mouse podocyte with compound **GFB-8438**, followed by incubation with PS, effectively blocked synaptopodin loss and cytoskeletal remodeling (Figure 3, C). This pharmacological effect is consistent with the prior study using tool TRPC5 inhibitor ML204,¹⁰ further validating the critical role of TRPC5 channel in maintaining podocyte cytoskeletal integrity.

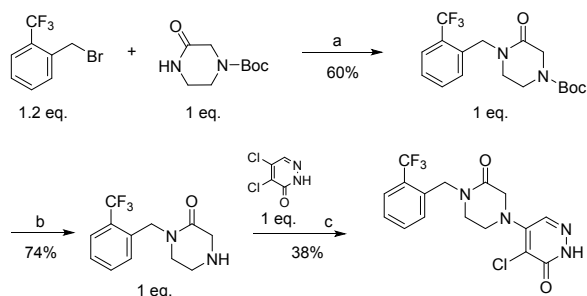
Next, **GFB-8438** was evaluated in an *in vivo* deoxycorticosterone acetate (DOCA)-rat model of FSGS. The DOCA-salt hypertensive rat is a well-established

model of mineralocorticoid hypertension with renal dysfunction, characterized by increased concentrations of urinary protein and albumin excretion.²² Based on the plasma exposure, we selected the highest tolerable subcutaneous dose of 30 mg/kg QD for this study. As shown in Figure 4, **GFB-8438** demonstrated robust benefits in this model. Statistically significant reduction in urine protein concentrations were seen after three weeks when compared to the DOCA control group. This trend was even more robust when analyzing the urine albumin concentrations, which were significantly lower at both two- and three-week timepoints and similar to the eplerenone control group. There was no significant difference in body weight in all treated groups. Animals receiving DOCA-**GFB-8438** did not exhibit significant differences in mean arterial blood pressure (BP), diastolic and systolic BP compared to DOCA group, while significant reduction of BP was observed at both week 2 and 3 in eplerenone treated group. The effect of **GFB-8438** on proteinuria without affecting blood pressure contrasts with mechanisms of action of angiotensin-converting enzyme (ACE) inhibitor or an angiotensin II receptor blocker (ARB) frequently used for the treatment of FSGS.

These data are consistent with TRPC₅ inhibitors such as **GFB-8438** having disease-modifying activity, addressing the pathogenesis of FSGS by protecting the integrity of the podocyte cytoskeleton.

The pyridazinone **GFB-8438** was efficiently prepared in a 3-step synthetic sequence described in Scheme 1 from commercially available starting materials. Standard alkylation of bromide with piperazinone under high temperature, followed by Boc deprotection and S_NAr reaction with 4,5-dichloropyridazinone furnished the synthesis of **GFB-8438** in overall 17% yield after recrystallization from acetic acid and water.

Scheme 1. Synthesis of Compound GFB-8438^a



^aReagents and conditions: (a) NaH (2 equiv), DMF, 0 °C to 110 °C; (b) TFA (7 equiv), DCM, 0 °C to rt; (c) DIEA (1.5 equiv), DMA, rt to 100 °C

In summary, starting from HTS screening hit **1**, a series of systematic medicinal chemistry SAR explorations led to the identification of **GFB-8438**, a novel, potent and subtype selective TRPC₅ inhibitor with favorable overall *in vitro* and *in vivo* properties. **GFB-8438** was shown to protect mouse podocytes from injury induced by protamine sulfate *in vitro*. More importantly, **GFB-8438** demonstrated robust efficacy in the hypertensive DOCA-salt rat model without affecting blood pressure, further validating the critical role of TRPC₅ channel in the pathogenesis of kidney disease.

Progress toward the identification of TRPC₅ inhibitors suitable for testing in clinical trials will be reported in due course.

ASSOCIATED CONTENT

Supporting Information

The Supporting Information is available free of charge on the ACS Publications website.

General chemistry methods; General Synthetic protocols; Synthetic procedures for the preparation of selected compounds; hTRPC₅ fluorescence-based assay (FLIPR) protocols; hTRPC₅ automated patch clamp assay (Qpatch) protocol; hTRPC₅ manual patch clamp assay protocol; automated patch clamp assay (Qpatch) protocol; hTRPC₆ automated patch clamp assay (Qpatch) protocol; Table S1.

DMPK profiling of **GFB-8438**, 32 and 35; Table S2. *In vitro* activity profile of **GFB-8438**; PS-induced mouse podocytes injury protection assay; Efficacy study in DOCA-salt rat model; Figure S1; References (PDF)

AUTHOR INFORMATION

Corresponding Author

*(M.L.) Tel: +1 (617) 337 4200. Email: mledeboer@goldfinchbio.com

*(M.Y.) Tel: +1 (617) 337 4200. Email: myu@goldfinchbio.com

Present Addresses

[▽](M.B.) Disc Medicine, 400 Tech Square, 10th floor, Cambridge, MA 02139, United States.

Author Contributions

The manuscript was written through contributions of all authors. All authors have given approval to the final version of the manuscript.

Notes

The authors declare the following competing financial interest(s): M.Y., M.W.L., M.D., G.M., T.T.T., M.C-L.G., X-R.P-Z., A.W-B., M.B., J.F.R., P.M., J-C.H are current or past employee of Goldfinch Bio Inc.

ACKNOWLEDGMENT

The authors would like to thank Liron Walsh, Adam Tebbe and Mark Duggan for assistance in manuscript preparation; Evotec for HTS screening; Pharmaron for chemical synthesis and DMPK support; Plato Biopharma for DOCA study; Icagen and SB Drug Discovery for assays support.

ABBREVIATIONS

FSGS, focal segmental glomerulosclerosis; CKD, chronic kidney disease; TRP, transient receptor potential; TRPC₅, TRP channel subfamily C, member 5; TRPA, TRP channel subfamily A; TRPV, TRP channel subfamily V; TRPM, TRP channel subfamily M; DOCA, deoxycorticosterone acetate; PS, protamine sulfate; CVD, cardiovascular disease; KO, knockout; LPS, lipopolysaccharide; ROS, reactive oxygen species; HTS, high throughput screening; SAR, structure activity relationship; CL, clearance; V_{ss}, volume of distribution; F, bioavailability; T_{1/2}, half-life; MDCK-MDR1, Madin-Darby Canine Kidney-multidrug resistance protein 1; ER, efflux ratio; hERG, human ether-a-go-go-related gene; HEK, human embryonic kidney; BP, blood pressure; S_NAr, nucleophilic aromatic substitution; SC, subcutaneous dose; PO, oral dose; DMPK, drug metabolism and pharmacokinetics; hLM, human liver microsomes; rLM, rat liver microsomes; DMF, dimethylformamide; TFA, trifluoroacetic acid; DCM, dichloromethane; DIEA, diisopropylethylamine; DMA, dimethylacetamide.

REFERENCES

- (1) Hill, N. R; Fatoba, S. T.; Oke, J. L.; O'Callaghan, C. A.; Lasserson, D. S.; Hobbs, F. D. R. Global prevalence of chronic kidney disease - a systematic review and meta-analysis. *PLoS ONE* **2016**, *11*, e0158765.
- (2) Coresh, J.; Selvin, E.; Stevens, L. A.; Manzi, J.; Kusek, J. W.;

Eggers, F. V. L.; Levey, A. S. Prevalence of chronic kidney disease in the United States. *JAMA*. **2007**, *298*, 2038–2047.

(3) Go, A. S.; Chertow, G. M.; Fan, D.; McCulloch, C. E.; Hsu, C. Y. Chronic kidney disease and the risks of death, cardiovascular events, and hospitalization. *N. Engl. J. Med.* **2004**, *351*, 1296–305.

(4) D'Agati, V. D.; Kaskel, F. J.; Falk, R. J. Focal segmental glomerulosclerosis. *N. Engl. J. Med.* **2011**, *365*, 2398–241.

(5) Greka, A.; Mundel, P. Cell biology and pathology of podocytes. *Annu. Rev. Physiol.* **2012**, *74*, 299–323.

(6) Yu, H.; Suleiman, H.; Kim, A. H. J.; Miner, J. H.; Dani, A.; Shaw, A. S.; Akilesh, S. Rac1 activation in podocytes induces rapid foot process effacement and proteinuria. *Mol. Cell. Biol.* **2013**, *33*, 4755–4764.

(7) Bezzerides, V.; Ramsey, I. S.; Kotecha, S.; Greka, A.; Clapham, D. E. Rapid vesicular translocation and insertion of TRP channels. *Nature Cell Biol.* **2004**, *6*, 709–720.

(8) Wieder, N.; Greka, A. Calcium, TRPC channels, and regulation of the actin cytoskeleton in podocytes: towards a future of targeted therapies. *Pediatr. Nephrol.* **2016**, *31*, 1047–1054.

(9) Montell C. The TRP Superfamily of cation channels. *Science's STKE*. **2005**, 272:re3

(10) Schaldecker, T.; Kim, S.; Tarabanis, C.; Tian, D.; Hakrrouch, S.; Castonguay, P.; Ahn, W.; Wallentin, H.; Heid, H.; Hopkins, C. R.; Lindsley, C. W.; Riccio, A.; Buwall, L.; Weins, A.; Greka, A. Inhibition of the TRPC5 ion channel protects the kidney filter. *J. Clin. Invest.* **2013**, *123*, 5298–5309.

(11) Zhou, Y.; Castonguay, P.; Sidhom, E-H.; Clark, A.R.; Dvela-Levitt, M.; Kim, S.; Sieber, J.; Wieder, N.; Jung, J. Y.; Andreeva, S.; Reichardt, J.; Dubois, F.; Hoffmann, S. H.; Basgen, J. M.; Montesinos, M. S.; Weins, A.; Johnson, A. C.; Lander, E. S.; Garrett, M. R.; Hopkins, C. R.; Greka, A. A small-molecule inhibitor of TRPC5 ion channels suppresses progressive kidney disease in animal models. *Science*, **2017**, *358*, 1332–1336.

(12) Minard, A.; Bauer, C. C.; Wright, D. J.; Rubaiy, H. N.; Muraki, K.; Beech, D.; Bon, R. S. Remarkable progress with small-molecule modulation of TRPC1/4/5 channels: implications for understanding the channels in health and disease. *Cells*, **2018**, *7*:52

(13) Rubaiy, H. N.; Ludlow, M. J.; Henrot, M.; Gaunt, H. J.; Miteva, K.; Cheung, S. Y.; Tanahashi, Y.; Hamzah, N. H.; Musialowski, K. E.; Blythe, N. M.; Appleby, H. L.; Bailey, M. A.; McKeown, L.; Taylor, R.; Foster, R.; Waldmann, H.; Nussbaumer,

P.; Christmann, M.; Bon, R. S.; Muraki, K.; Beech, D. J. Picomolar, selective, and subtype-specific small-molecule inhibition of TRPC1/4/5 channels. *J. Biol. Chem.* **2017**, *292*, 8158–8173.

(14) Rubaiy, H. N. Treasure troves of pharmacological tools to study transient receptor potential canonical 1/4/5 channels. *Br. J. Pharmacol.* **2019**, *176*, 832–846.

(15) Miller, M.; Shi, J.; Zhu, Y.; Kustov, M.; Tian, J-B.; Stevens, A.; Wu, M.; Xu, J.; Long, S.; Yang, P.; Zholos, A-V.; Salovich, J. M.; Weaver, C.D.; Hopkins, C. R.; Lindsley, C. W.; McManus, O.; Li, M.; Zhu, M. X. Identification of ML204, a novel potent antagonist that selectively modulates native TRPC4/C5 ion channels. *J. Biol. Chem.* **2011**, *286*, 33436–33446.

(16) Richter, J. M.; Schaefer, M.; Hill, K. Clemizole hydrochloride is a novel and potent inhibitor of transient receptor potential channel TRPC5. *Mol. Pharmacol.* **2014**, *86*, 514–521.

(17) Sharma, S. H.; Pablo, J. L.; Montesinos, M. S.; Greka, A.; Hopkins, C. R. Design, synthesis and characterization of novel N-heterocyclic-1-benzyl-1Hbenzo[d]imidazole-2-amines as selective TRPC5 inhibitors leading to the identification of the selective compound, AC1903. *Bioorg. Med. Chem. Lett.* **2019**, *29*, 155–159.

(18) Just, S.; Chenard, B. L.; Cecii, A.; Strassmaier, T.; Chong, J. A.; Blair, N. T.; Gallaschun, R. J.; Camino, D.; Cantin, S.; D'Amours, M.; Eickmeier, C.; Fanger, C. M.; Hecker, C.; Hessler, D. P.; Hengerer, B.; Kroker, K. S.; Malekiani, S.; Mihalek, R.; McLaughlin, J.; Rast, G.; Witek, J.; Sauer, A.; Pryce, C. R.; Moran, M. M. Treatment with HC-070, a potent inhibitor of TRPC4 and TRPC5, leads to anxiolytic and antidepressant effects in mice. *PLoS ONE* **2018**, *13*, e0191225.

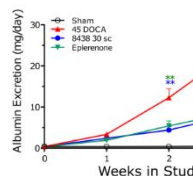
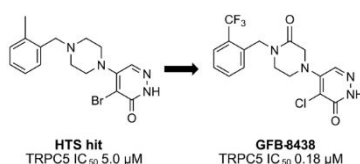
(19) Hernandez, M. Z.; Cavalcanti, S. M.; Moreira, D. R.; de Azevedo Junior, W. F.; Leite, A. C. Halogen atoms in the modern medicinal chemistry: hints for the drug design. *Curr. Drug Targets*. **2010**, *11*, 303–314.

(20) Buwall, L.; Wallentin, H.; Sieber, J.; Andreeva, S.; Choi, H. Y.; Mundel, P.; Greka, A. *J. Am. Soc. Nephrol.* **2017**, *28*, 837–851.

(21) Tian, D.; Jacobo, S. M.; Billing, D.; Rozkalne, A.; Gage, S. D.; Anagnostou, T.; Pavenstädt, H.; Hsu, H. H.; Schlondorff, J.; Ramos, A.; Greka, A. Antagonistic regulation of actin dynamics and cell motility by TRPC5 and TRPC6 channels. *Sci Signal* **2010**, *3*: ra77

(22) Schenk, J.; McNeill, J. H. The pathogenesis of DOCA-salt hypertension. *J. Pharmacol. Toxicol. Methods* **1992**, *27*, 161–170.

Insert Table of Contents artwork here



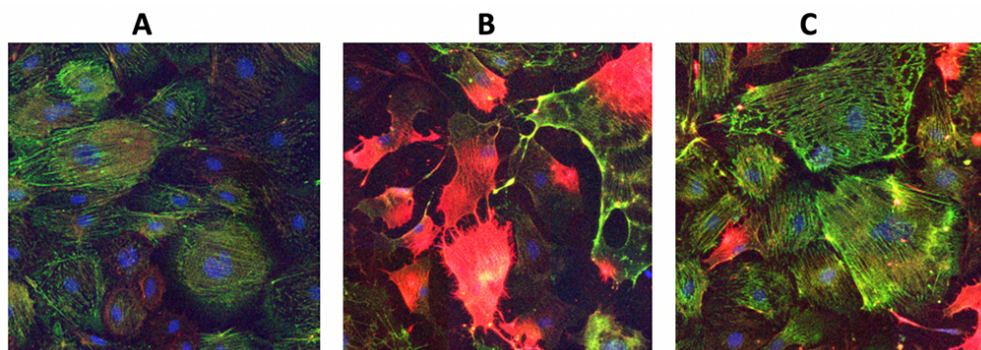


Figure 3. in vitro efficacy study for GFB-8438 in PS-induced mouse podocytes injury assay

86x30mm (300 x 300 DPI)

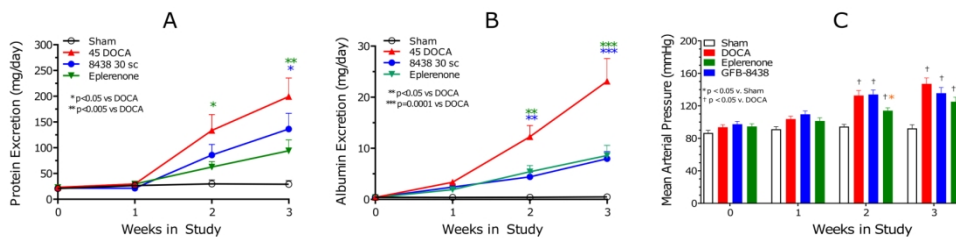
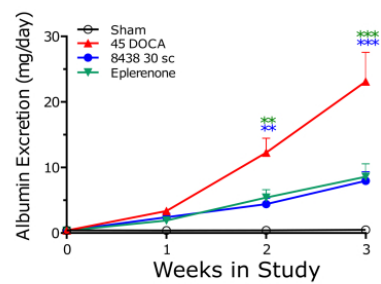
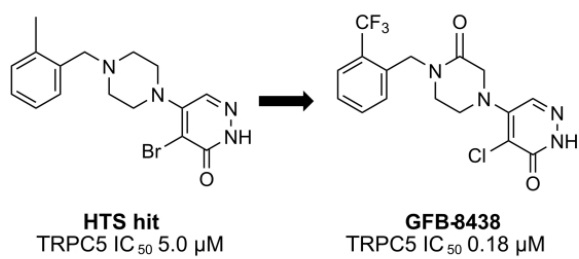


Figure 4. in vivo efficacy study for GFB-8438 in DOCA rat model

158x37mm (300 x 300 DPI)



TOC

82x27mm (300 x 300 DPI)